Comparison of two innovative precipitation systems for ZnO and Al-doped ZnO nanoparticle synthesis

Anne Aimable[1,*], Tomasz Strachowski[2], Ewelina Wolska[2,3], Witold Lojkowski[2], Paul Bowen[1]

[1]*Powder Technology Laboratory (LTP), Materials Institute, Swiss Federal Institute of Technology, Ecole Polytechnique Fédérale de Lausanne (EPFL), 1015 Lausanne, Switzerland*

[2]*High Pressure Physics Centre of the Polish Academy of Science, Sokolowska 29/37, Warsaw, Poland*

[3]*Institute of Physics, Polish Acad. of Sciences, Al. Lotników 32/46, 02-668 Warsaw, Poland*

Received 9 February 2010; received in revised form 23 August 2010; accepted 27 August 2010

Abstract

This study presents a comparative approach to investigate the potentials of two innovative methods for the synthesis of ZnO and Al-doped ZnO. The first method is a precipitation system working in mild hydrothermal conditions (90°C) using a tubular reactor (Segmented Flow Tubular Reactor, SFTR). The second method is a microwave-assisted hydrothermal process working at 250°C - 38 atmospheres. Nanocrystalline ZnO with a high specific surface area (49–68 m²/g) was obtained with both systems. Smaller equiaxed particles (50–70 nm) were obtained with the SFTR, with an excellent homogeneity in size and morphology, which was attributed to an excellent control of the process parameters (mixing, temperature, volume of reaction). A higher luminescence signal was measured on these samples. The microwave method leads to particles with a higher crystallinity due to the temperature of the reaction. A significant effect of the aluminum was observed, which reduces the crystal growth to produce equiaxed morphologies. This effect was enhanced by adding poly(acrylic) acid (PAA).

Keywords*: ZnO, precipitation, particle size distribution, photoluminescence*

I. Introduction

Nanomaterials attract the interest of the international research because they open new fascinating perspectives in many applications domains [1]. However new generations of devices will depend on the availability of these nanomaterials at an industrial scale. The low-cost production of such advanced nanocrystals with well-defined electronic, optoelectronic and catalytic properties still remains a big challenge, and strong efforts are being carried out on the development of more efficient and reliable synthesis processes.

This paper compares two innovative methods for the synthesis of zinc oxide nanoparticles, pure or Al-doped. The first one is a precipitation system in mild hydrothermal conditions (90°C) using a tubular reactor the Segmented Flow Tubular Reactor (SFTR) [2]. Tubular reactors, when compared with batch reactors, are of great interest for powder production targets because they can easily be operated under a continuous mode. The Segmented Flow Tubular Reactor, or SFTR, has been developed to overcome the classical problems of powder production scale-up from batch processes. By generating identical micro-reactors giving a homogeneous mixing of the reactants, the SFTR avoids poor mixing and inhomogeneous reaction conditions often encountered in classical large batch reactors. This process has proved its versatility and its robustness through the preparation of several different products ($CaCO_3$ [3], $BaTiO_3$ [4], oxalates [5,6]) assuring a high powder quality (chemical and phase composition, particle size, and shape) and reproducibility over time. The transfer of the laboratory conditions to an industrial scale of production can easily be achieved by multiplying the number of individual tubular reactors running in parallel - that is to say to "scale-out" rather than "scale-up" [7,8].

Zinc oxide nanoparticles were also synthesized through a hydrothermal route, using a microwave heat-

* Corresponding author: tel: +41 21 693 51 09
fax: +41 21 693 30 89, e-mail: *anne.aimable@epfl.ch*

ing. This process has significant advantages over conventional hydrothermal reactions, where the limiting step is mainly the heat transfer between the furnace, reactor, and reaction mixture [9]. It allows considerably faster heating rates, leading to a higher degree of crystallinity of the materials, and higher nucleation rates, leading to the formation of finer solid particles [10–12].

Zinc oxide is a very popular material, having a wide range of applications in ceramics, coatings, and electronic devices. It is an II-IV semiconductor, with a wide band-gap (3.37 eV at room temperature), and a large exciton binding energy (60 meV). These particular features make ZnO one of the most promising candidates for room temperature UV lasers and short-wavelength optoelectronic devices. Some detailed reviews have appeared in recent years, dedicated to ZnO synthesis [13], its electronic properties [14], applications of ZnO as varistors [15], quantum dots [16] and photonic devices [17].

Al-doped ZnO compounds are well-known materials used as transparent conductive oxides (TCOs) for transparent electrodes in electronic devices [18–20], or as thermal insulator films in low emissive windows [21]. The aluminum doping of ZnO is an n-type doping, resulting in ZnO films with a higher conductivity [22]. Al-doped nanoparticles exhibit a higher optical band-gap [23] and a higher luminescence is observed for an optimum Al concentration depending on the synthesis process [11,24]. In this study aluminum was added as a dopant in both synthesis systems, and the luminescence of the powders was measured and compared.

II. Materials and Methods

2.1 Mild-hydrothermal precipitation: SFTR

Zinc oxide nanoparticles were produced by precipitation in mild hydrothermal conditions by using the Segmented Flow Tubular Reactor (SFTR). A schematic view of the SFTR is given in Fig. 1. It is composed of three distinct parts: a micromixer, a segmenter, and a tubular reactor placed in a thermostatic bath at 90°C. The reactants are introduced through the micromixer where the initial supersaturation is created. The mixing time is estimated around 10 ms [25]. The reacting mixture is then segmented by an immiscible solvent: dodecane in the case of ZnO precipitation. Thus small suspension volumes (~ 0.2 cm^3) are created, which can be assimilated to microreactors, where the precipitation and growth takes place. The time of the reaction is determined by the pump speed and the tube length, and is around 10 minutes in the considered reaction. This process is in a steady-state situation in which each step, mixing and ageing, is well separated, leading to a better control and reproducibility. After the tubular reactor, a heat-exchanger is placed to stop the reaction, and cool down the reacting mixture to room temperature. Then a decanter allows the separation of the aqueous suspension and the immiscible fluid. The powder in the aqueous phase is collected, while the dodecane is recycled in the process for environmental and cost considerations.

The precipitation of ZnO results from the mixing of zinc nitrate and sodium hydroxide aqueous solutions. The Zn^{2+} reaction solution at 0.10 M was prepared by dissolving $Zn(NO_3)_2{\times}6H_2O$ in ultra pure water. Aluminium nitrate ($Al(NO_3)_3{\times}9H_2O$) was introduced in the zinc nitrate solution in different amounts for Al-doping: Al/Zn molar ratios were 0.5% and 1.0%. The NaOH reaction solution at 0.11 M was prepared by diluting a titrated solution NaOH 1 M in ultra pure water. Poly(acrylic acid) (PAA M_w 2000) at 0.05 wt.% is added in the NaOH reaction solution for a better control of the precipitated powder [26]. After reaction, the suspended powder is washed 4 times with ultra pure water, before being filtered and dried for 24 hours at 70°C.

2.2 Microwave-assisted hydrothermal precipitation

The microwave-assisted hydrothermal precipitation was conducted using a home-made stop-flow reactor. This equipment allows an automatic pumping of the precursor into a batch reactor of 250 mL, and can deliver a maximum heating power of 1000 W. Zinc hydroxide $Zn(OH)_2$ was prepared by adding KOH 5.0 M to a solution of $Zn(NO_3)_2{\times}6H_2O$ 1.0 M at room temperature until the pH reaches 10. Aluminium nitrate ($Al(NO_3)_3{\times}9H_2O$) was introduced in the zinc nitrate solution in different amounts for Al-doping: Al/Zn molar ratios were 0.05 and 0.10. Some poly(acrylic acid) (PAA M_w2000) at 0.025 wt.% was also introduced to study its influence on ZnO precipitation. This precursor was then transferred to the microwave-assisted hydrothermal re-

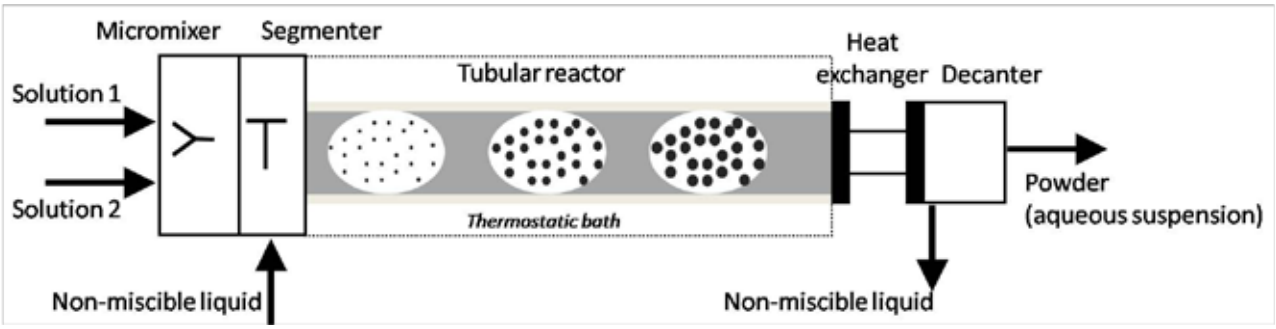

Figure 1. Schematic views of the Segmented Flow Tubular Reactor (SFTR)

actor, and heated at 38 atmospheres at 250°C during 30 minutes. After the process completion, the product obtained was washed 4 times with ultra pure water, before being filtered and dried for 24 hours at 70°C.

2.3 Powder characterization

The phase identification of the precipitates was made with powder X-ray diffraction (XRD, Philips X'Pert diffractometer, Cu-K_α radiation). XRD peak broadening was used to determine the size of the primary crystallite using the Scherrer equation (Eq. 1). The instrumental broadening was determined using alumina with a large crystal size (> 1 μm).

$$d_{XRD} = \frac{K \cdot \lambda_X}{\beta_{X_p} \cdot \cos(\theta)} \quad (1)$$

where K is equal to 0.9 [27], λ_X is the X-ray wavelenght, β_{Xp} is the integral breadth of the material, calculated using $\beta_{Xp} = \sqrt{(\beta^2 - \beta^2_{alumina})}$, and β the integral breadth is the ratio of the area and the height of the diffraction peak.

The powder morphologies were analyzed by scanning electron microscopy (SEM, Philips XL 30 FEG microscope). The SEM samples were prepared by dispersing the powder in ethanol. One drop of the suspension was then deposited on an aluminum support and dried in air. TEM micrographs were obtained from a Philips CM 200 TEM operating at 200 kV at room temperature.

The density of the powder was measured with Helium pycnometry (Micromeritics Acoupyc 1330). Before the measurement the samples were dried at 200°C in air for 1 h.

Brunauer-Emmett-Teller (BET) specific surface areas S_{BET} (m^2g^{-1}) were estimated from N_2 adsorption isotherms (Micromeritics Gemini 2375). The size of the primary particles, d_{BET} (nm), were calculated by assuming spherical monodisperse particles (Eq. 2), with ρ the density of the material measured by pycnometry.

$$d_{BET} = \frac{6000}{S_{BET} \cdot \rho} \quad (2)$$

Before BET measurements the samples were dried at 200°C in flowing nitrogen for 1 h.

The actual content of Zn and Al in the powder was determined by Inductively Coupled Plasma - Optical Emission Spectroscopy (ICP-OES, Perkin Elmer Optima 3300).

The particle size distribution (PSD) was collected using a centrifugal method (CPS, Disc Centrifuge Model DC 24000). Thermogravimetric curves (TGA, Mettler TGA/DSC/TMA analyzer) were collected from room temperature to 800°C under flowing air at a heating rate of 10 °C/min.

Photoluminescence (PL) was measured at room temperature, using Spectrofluorimeter CM2203 (Solar) with a 150 W high pressure Xe lamp. Both slits (excitation and detection) of the monochromator were set at 5 nm optical width. The sample was excited at 300 nm wavelength, and photoluminescence was measured from 340 nm to 820 nm.

III. Results and discussion

The powders characteristics are presented in Table 1. Powders synthesized via the SFTR show a well-defined diffractogram matching the ZnO pattern of wurtzite (ICDD 075-0576) whatever the aluminium content (Fig. 2). The precursor mixture prepared at room temperature for the assisted-microwave hydrothermal treatment is a poorly crystalline phase composed of $Zn(OH)_2$, ZnO, and $Al(OH)_3$ when aluminium nitrate is added as a dopant. After the microwave-assisted hydrothermal treatment crystalline ZnO is formed. However the XRD diffractogram of the doped sample MW-Al0.05 shows some small peaks that have been attributed to the spinel phase $ZnAl_2O_4$ (stars in the diagram). Because of the small intensity of those peaks, it is really difficult to ensure that this phase has not been formed in the other doped samples with the microwave method (MW-Al0.1, MW-Al0.05-PAA). It would be in agreement with recent papers showing that the solubility limit of Al in ZnO is very low (1 to 3% depending on the authors [28,29]) before $ZnAl_2O_4$ appears as a second phase.

The ICP-OES analysis (Table 1) shows that the aluminum has been incorporated in all doped powders. Af-

Table 1. Results of Al/Zn by ICP-OES, d_{XRD}, S_{BET}, d_{BET}, and weight loss measured by TGA, of ZnO and Al-doped ZnO powders obtained with the SFTR and the microwave-assisted hydrothermal process

Sample code		As-synthesized powder						10 min – 450°C	
Method	Al/Zn ratio-additive	Al/Zr by ICP-OES	d_{XRD} [nm]	S_{BET} [m^2/g]	density [g/cm^3]	d_{BET} [nm]	Weight loss TGA [%]	S_{BET} [m^2/g]	density [g/cm^3]
SFTR	Al0-PAA	0	24	68	4.07	22	13.3	21	5.10
	Al0.005-PAA	0.01	22	66	4.08	22	14.4	29	5.09
	Al0.01-PAA	0.02	25	62	4.02	24	15.7	26	5.18
MW	Al0	0	38	7	5.46	157	1.6		
	Al0.05	0.05	35	18	5.07	66	4.7		
	Al0.1	0.10	30	39	4.99	31	5.3		
	Al0.05-PAA	0.05	22	49	4.71	26	8.0		

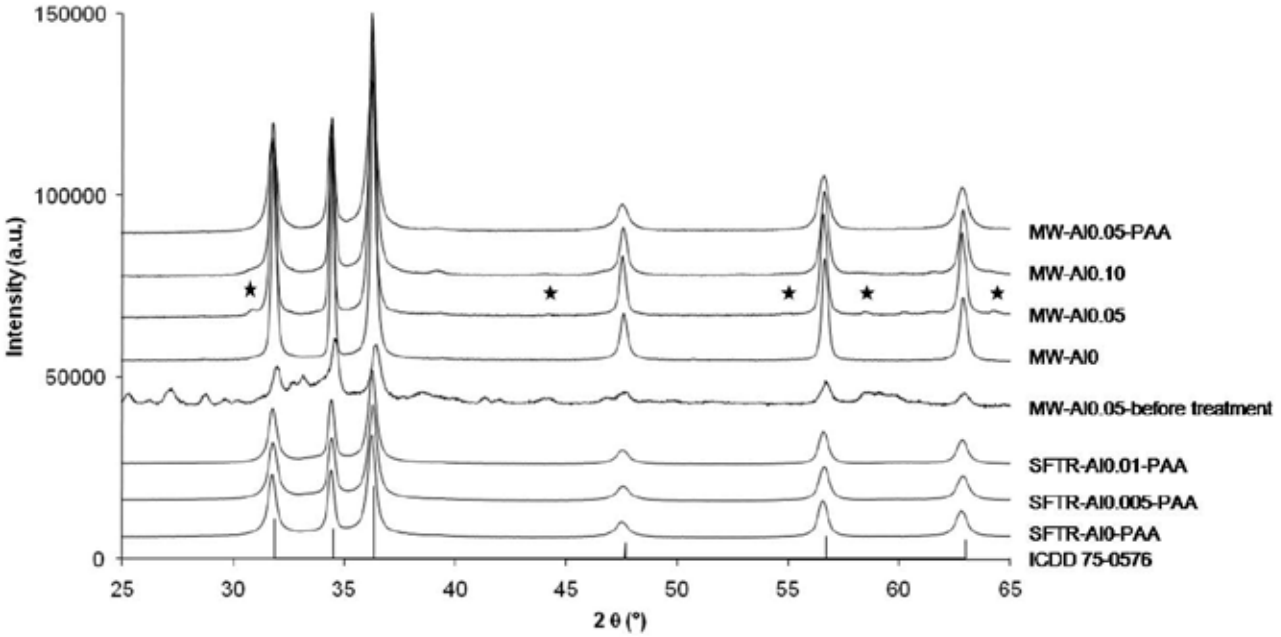

Figure 2. XRD patterns of ZnO and Al-doped ZnO powders synthesized with the SFTR and the microwave-assisted hydrothermal process (* $ZnAl_2O_4$)

ter a mild-hydrothermal reaction with the SFTR, the Al/Zn molar ratio in the powder is twice the initial ratio in the reactive solution. It is coherent with the thermodynamic conditions and our experimental observations, where only 53 at.% of the zinc was precipitated, and 47 at.% remained as soluble Zn species (Zn^{2+} and $Zn(OH)^{+}$) [26]. Therefore we can conclude that all the aluminum introduced in the reactive solution has been incorporated into the precipitated powder. After the assisted-microwave hydrothermal process the same content of aluminium is measured in the powder to that in the reactive mixture. However the way the aluminum is incorporated is still unknown, and is the subject of our current research.

Crystallite sizes of powders were calculated using the [100] reflection and are given in Table 1. Zinc oxide precipitated by microwave-assisted hydrothermal process without aluminium or polymeric additive presents a crystallite size of 38 nm. By adding aluminum the crystallite size is slightly decreased towards 30 nm for Al/Zn = 0.10. By adding PAA, the crystallite size is decreased further to 22 nm. Similar effects have been observed on ZnO powders synthesized in mild-hydrothermal conditions [26]. The crystallite sizes of samples obtained with the SFTR with PAA and Al are in the same range (22 to 25 nm). Therefore both processes allow the synthesis of Al-doped ZnO nanocrystals, and for both an inhibition of the crystal growth is observed in presence of PAA.

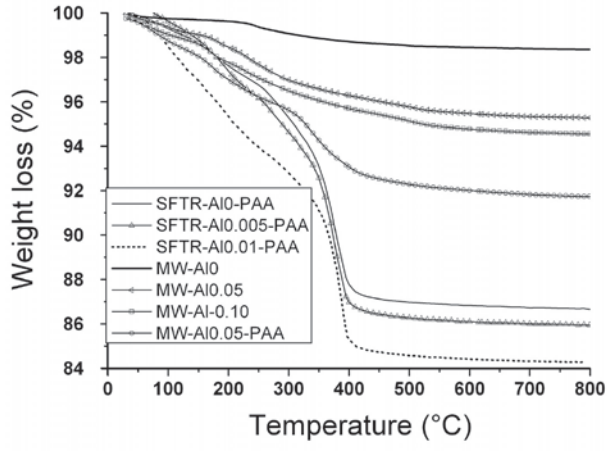

Figure 3. TG curves obtained for ZnO and Al-doped ZnO powders synthesized with the SFTR and the microwave -assisted hydrothermal process (heating rate 10 °C/min in flowing air 30 mL/min)

All powders obtained with the SFTR show very high specific surface areas (62 to 68 m^2/g), whatever the aluminum content. After elimination of PPA by a heat treatment of 10 minutes at 450°C, the specific surface area is decreased to 21–28 m^2/g. MW-Al0 from the microwave-assisted hydrothermal process presents a lower surface area of 7 m^2/g. The addition of aluminum as a dopant leads to a significant increase of the specific surface area, to 39 m^2/g with Al/Zn = 0.10, and the further addition of PAA leads to a further increase to 49 m^2/g.

The analysis of TGA curves (Fig. 3) show that PAA is strongly adsorbed at the surface of ZnO. The first weight loss between 30 and 200°C was attributed to the removal of physically adsorbed water. The second weight loss between 200 and 400°C is the consequence of two phenomena: the decomposition of chemically bound hydroxyl groups, and the removal of the organic compound. A higher amount of PAA is adsorbed at the surface of samples obtained with the SFTR, which can be related to the higher specific surface area of those samples.

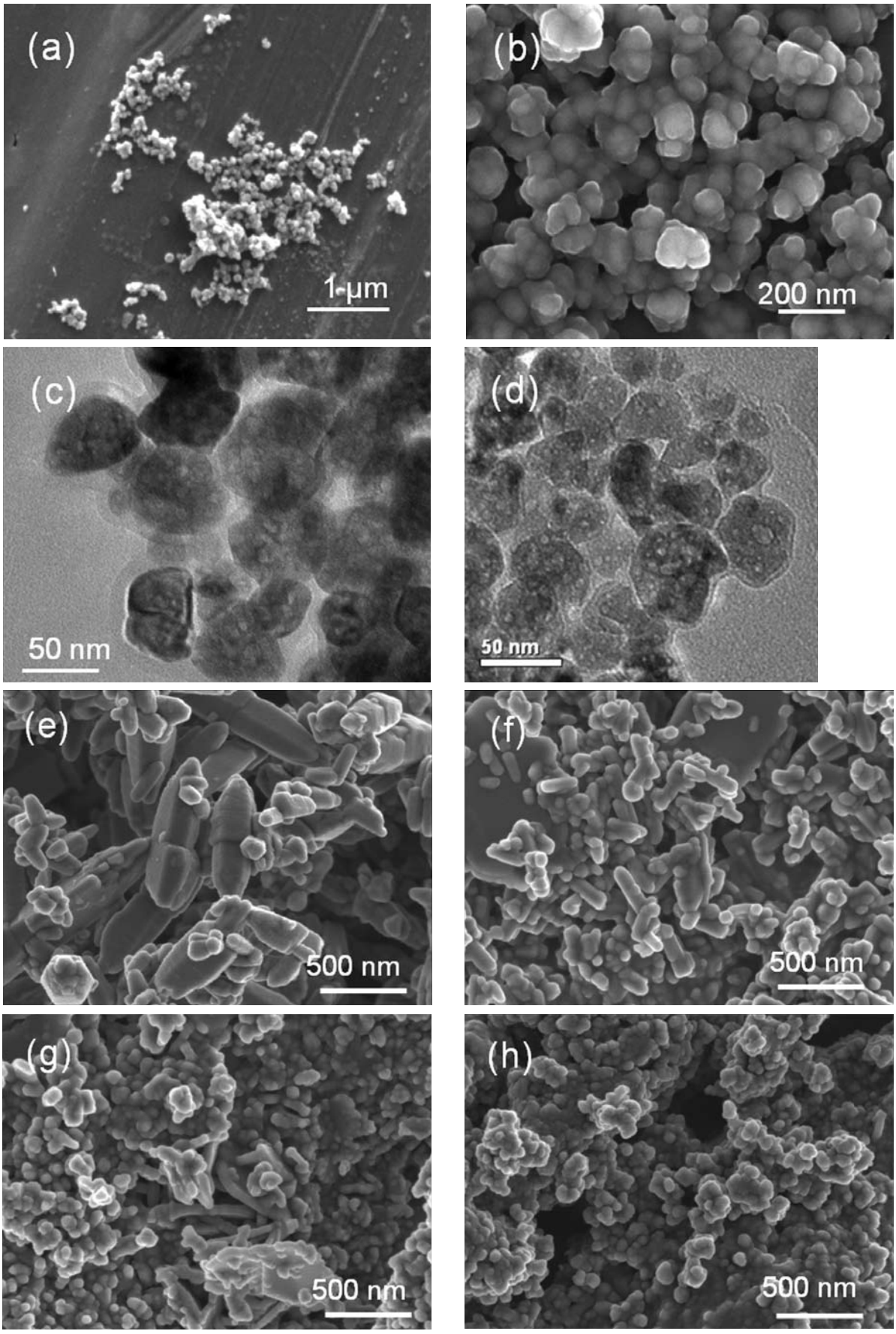

Figure 4. SEM and TEM micrographs of ZnO and Al-doped powders from different synthesis conditions (a,b,c) SFTR-Al0-PAA, (d) SFTR-Al0.005-PAA, (e) MW-Al0, (f) MW-Al0.05, (g) MW-Al0.10, (h) MW-Al0.05-PAA

The powder density was measured by helium pycnometry. The density of MW-Al0 (d = 5.46, Table 1) is close to the theoretical density of ZnO (d =5.606), which indicates a good crystallinity of this material. The addition of aluminium leads to a slight decrease of the density. This could indicate that Al is incorporated into the crystal lattice (lower molecular weight of Al: 27 g/mol, compared to Zn: 65 g/mol), however further research needs to be pursued to confirm this. The density of MW-Al0.05-PAA is lower than MW-Al0.05 because of the presence of the adsorbed polymer. Also in mild-hydrothermal conditions low densities around 4 were measured, which were explained by a lower crystallinity and a higher amount of adsorbed PAA. Thus after a heat-treatment, densities around 5.1 were obtained for these samples. No effect of the aluminum content was observed certainly due to the very low concentration as measured by ICP-OES.

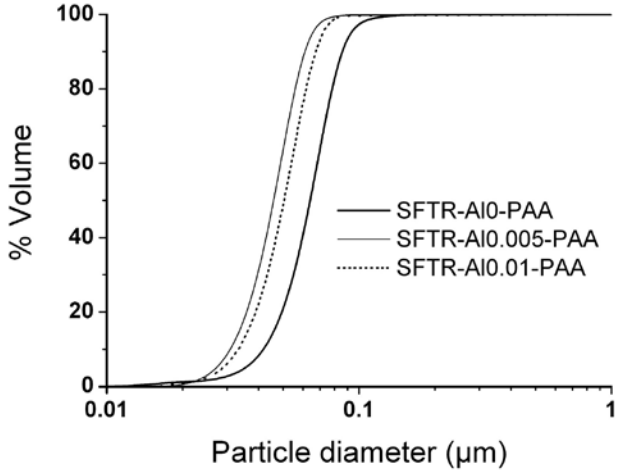

Figure 5. Particle size distributions of ZnO and Al-doped ZnO powders synthesized with the SFTR, measured by centrifugal sedimentation (CPS)

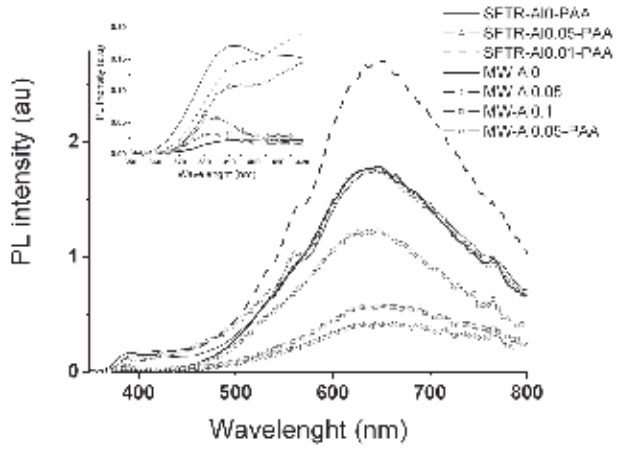

Figure 6. Room temperature photoluminescence (PL) spectra of ZnO and Al-doped ZnO powders synthesized with the SFTR and the microwave-assisted hydrothermal process (excitation: 300 nm). Inset is an expanded scale for the 350 to 420 nm section of the spectra

From SEM observations, the SFTR process produces particles homogeneous in size, with a narrow particle size distribution (PSD) and equiaxed morphologies (Fig. 4a-d). The mean particle size of SFTR-Al0-PAA measured from a centrifugal method is d_{v50} = 64 nm (Fig. 5). The addition of a very small amount of aluminium (Al/Zn = 0.01) leads to a decrease to d_{v50} = 46 nm. The power of the SFTR is that it allows a continuous production of very homogeneous ZnO nanocrystals, in a very reproducible way [24]. The current investigation shows that this behaviour can be extended to Al-doped ZnO with different Al contents. Nanoparticles are also formed via the microwave-assisted hydrothermal method, as shown in Fig. 4e-h. By adding some aluminium the elongation observed in many particles of MW-Al0 is reduced. The addition of PAA also inhibits the elongated growth leading to smaller and more homogeneous particles (150–200 nm) with equiaxed morphologies. Without any additive or dopant the microwave-assisted hydrothermal method seems to lead to a chaotic nucleation and growth, leading to less control on the final particle size and PSD than when using the SFTR. This is mainly explained by the use of a micromixer in the SFTR, which controls the initial supersaturation, and the smaller reaction volume (~0.2 cm^3 for each droplet) which ensures a more homogeneous heating and concentration profile.

Photoluminescence spectra were recorded on the different samples (Fig. 6). All of them show a characteristic peak at 380–385 nm, and a wide green to red band (500–800 nm) typical of defects in the material [30,31]. The magnified spectra between 340–420 nm shows that the powders synthesized via the SFTR present a higher luminescence signal, the intensity is 2 to 3 times higher than the intensity measured on microwave samples. For the SFTR samples, the addition of aluminum does not improve the luminescence around 380 nm, but increases the intensity of the broad band, presumably because more defects such as oxygen vacancies are created. For the samples synthesized by using the microwave method, there is a significant increase of the intensity of the signal around 380 nm by adding aluminum, whereas the intensity of the broad band is lower.

IV. Conclusions

This comparative approach has been very useful to investigate the potentials of two innovative methods for the synthesis of nanocrystalline ZnO and Al-doped ZnO. The microwave-assisted hydrothermal process presents the advantage of directly forming a fully-crystalline powder because of a higher temperature (250°C). A better control of the size and the morphology is obtained by adding aluminum as well as poly(acrylic) acid (PAA), and equiaxed particles (150–200 nm) were finally obtained with a high specific surface area (49 m^2/g, indicative of primary particles of around 25 nm). The mild-hydrothermal precipitation with the SFTR al-

lows the synthesis of nanoparticles with a higher specific surface area (68 m^2/g) and an excellent homogeneity in size and shape, in a continuous and reproducible way. This is mainly attributed to a better design of the process itself with a very good control of the process parameters (mixing, temperature, volume of reaction etc.) which are essential in precipitation. Higher intensity of the luminescence was measured on the SFTR samples. From this study it seems that a small amount of aluminium (up to 1%) could be incorporated inside the ZnO structure, whereas with more aluminium a second phase, $ZnAl_2O_4$, starts to precipitate. However the way the aluminum is incorporated (inside the crystal, or segregated at the surface and/or at grain boundaries) is still unknown, and is the subject of our current research.

Acknowledgements: The authors would like to acknowledge the COST Action 539 and the Swiss Costs office for support and funding.

References

1. P. Rodgers, *Nanoscience and Technology*, World Scientific Publishing, 2009.
2. J. Lemaitre, N. Jongen, R. Vacassy, P. Bowen, "Production of powders", *U.S. Patent 6458335*, Octobre 1, 2002.
3. R. Vacassy, J. Lemaitre, H. Hofmann, J.H. Gerlings, "Calcium carbonate precipitation using new segmented flow tubular reactor", *AIChE J.,* **46** (2000) 1241–1252.
4. P. Bowen, M. Donnet, A. Testino, M. Viviani, M.T. Buscaglia, V. Buscaglia, P. Nanni, "Synthesis of barium titanate powders by low-temperature aqueous synthesis using a new segmented flow tubular reactor", *Key Eng. Mater.*, **206-213** (2002) 21–24.
5. S. Guillemet-Fritsch, M. Aoun-Habbache, J. Sarrias, A. Rousset, N. Jongen, M. Donnet, P. Bowen, J. Lemaitre, "High-quality nickel manganese oxalate powders synthesized in a new segmented flow tubular reactor", *Solid State Ionics*, **171** (2004) 135–140.
6. M. Donnet, N. Jongen, J. Lemaître, P. Bowen, "New morphology of calcium oxalate trihydrate precipitated in a segmented flow tubular reactor", *J. Mater. Sci. Lett.*, **19** (2000) 749–750.
7. P. Bowen, A. Testino, V. Legagneur, M. Donnet, H. Hofmann, N. Cobut, "Precipitation of nanostructured and ultrafine powders: Process intensification using the segmented flow tubular reactor (SFTR) - still in search of the perfect powder?" in *Proceedings of Fifth World Congress on Particle Technology (WCPT5)*, Orlando, USA, 2006.
8. N. Jongen, M. Donnet, P. Bowen, J. Lemaitre, H. Hofmann, R. Schenk, C. Hofmann, M. Aoun-Habbache, S. Guillemet-Fritsch, J. Sarrias, A. Rousset, M. Viviani, M. Buscaglia, V. Buscaglia, P. Nanni, A. Testino, J. Herguijuela, "Development of a continuous segmented flow tubular reactor and the scale-out concept - In search of perfect powders", *Chem. Eng. Technol.*, **26** (2003) 303–305.
9. E.T. Thostenson, T-. Chou, "Microwave processing: fundamentals and applications", pp. 1055–1071 in *Composites Part A: Appl. Sci. Manufacturing,* **30** (1999) 1035-1071.
10. A. Shaporev, V. Ivanov, A. Baranchikov, Y. Tret'yakov, "Microwave-assisted hydrothermal synthesis and photocatalytic activity of ZnO", *Inorg. Mater.*, **43** (2007) 35–39.
11. T. Strachowski, E. Grzanka, W. Lojkowski, A. Presz, M. Godlewski, S. Yatsunenko, H. Matysiak, R.R. Piticescu, C.J. Monty, "Morphology and luminescence properties of zinc oxide nanopowders doped with aluminum ions obtained by hydrothermal and vapor condensation methods", *J. Appl. Phys.*, **102** (2007) 073513-9.
12. R.R. Piticescu, R.M. Piticescu, C.J. Monty, "Synthesis of Al-doped ZnO nanomaterials with controlled luminescence", *J. Eur. Ceram. Soc.*, **26** (2006) 2979–2983.
13. Z.L. Wang, "Zinc oxide nanostructures: growth, properties and applications", *J. Phys.: Condensed Matter*, **16** (2004) R829–R858.
14. U. Ozgur, Y.I. Alivov, C. Liu, A. Teke, M.A. Reshchikov, S. Dogan, V. Avrutin, S. Cho, H. Morkoc, "A comprehensive review of ZnO materials and devices", *J. Appl. Phys.*, **98** (2005) 041301-103.
15. D.R. Clarke, "Varistor ceramics", *J. Am. Ceram. Soc.*, **82** (1999) 485–502.
16. V.A. Fonoberov, A.A. Balandin, "ZnO quantum dots: Physical properties and optoelectronic applications", *J. Nanoelectron. Optoelectron.*, **1** (2006) 19–38.
17. M. Willander, O. Nur, Q.X. Zhao, L.L. Yang, M. Lorenz, B.Q. Cao, J. Zúñiga Pérez, C. Czekalla, G. Zimmermann, M. Grundmann, A. Bakin, A. Behrends, M. Al-Suleiman, A. El-Shaer, A. Che Mofor, B. Postels, A. Waag, N. Boukos, A. Travlos, H.S. Kwack, J. Guinard, D. Le Si Dang, "Zinc oxide nanorod based photonic devices: recent progress in growth, light emitting diodes and lasers", *Nanotechnol.*, **20** (2009) 332001.
18. G.G. Valle, P. Hammer, S.H. Pulcinelli, C.V. Santilli, "Transparent and conductive ZnO:Al thin films prepared by sol-gel dip-coating", *J. Eur. Ceram. Soc.*, **24** (2004) 1009–1013.
19. V.A. Fonoberov, A.A. Balandin, "ZnO Quantum Dots: Physical Properties and Optoelectronic Applications", *J. Nanoelectron. Optoelectron.*, **1** (2006) 19–38.
20. T. Schuler, M.A. Aegerter, "Optical, electrical and structural properties of sol gel ZnO:Al coatings", *Thin Solid Films*, **351** (1999) 125–131.
21. Z. Jin, I. Hamberg, C.G. Granqvist, "Optical properties of transparent and heat reflecting ZnO:Al films made by reactive sputtering", *Appl. Phys. Lett.*, **51** (1987) 149–151.
22. M. Chen, Z.L. Pei, C. Sun, L.S. Wen, X. Wang, "Surface characterization of transparent conductive oxide Al-doped ZnO films", *J. Crystal Growth*, **220** (2000) 254–262.

23. S. Suwanboon, P. Amornpitoksuk, A. Haidoux, J. Tedenac, "Structural and optical properties of undoped and aluminium doped zinc oxide nanoparticles via precipitation method at low temperature", *J. Alloys Compd.*, **462** (2008) 335–339.
24. K. Chen, T. Fang, F. Hung, L. Ji, S. Chang, S. Young, Y. Hsiao, "The crystallization and physical properties of Al-doped ZnO nanoparticles", *Appl. Surf. Sci.*, **254** (2008) 5791–5795.
25. A. Aimable, N. Jongen, A. Testino, M. Donnet, J. Lemaître, H. Hofmann, P. Bowen, "Precipitation of nanosized and nanostructured powders: process intensification and scale-out using the Segmented Flow Tubular Reactor (SFTR) for $BaTiO_3$, $CaCO_3$ and ZnO", *Chem. Eng. Technol.*, submitted.
26. A. Aimable, M.T. Buscaglia, V. Buscaglia, P. Bowen, "Polymer-assisted precipitation of ZnO nanoparticles with narrow particle size distribution," *J. Eur. Ceram. Soc.*, **30** (2010) 591–598.
27. J.I. Langford, A.J.C. Wilson, "Scherrer after sixty years: A survey and some new results in the determination of crystallite size", *J. Appl. Crystallogr.*, **11** (1978) 102–113.
28. D. Nie, T. Xue, Y. Zhang, X. Li, "Synthesis and structure analysis of aluminum doped zinc oxide powders", *Sci. China Series B: Chem.*, **51** (2008) 823–828.
29. H. Serier, M. Gaudon, M. Ménétrier, "Al-doped ZnO powdered materials: Al solubility limit and IR absorption properties," *Solid State Sci.*, **11** (2009) 1192–1197.
30. K. Vanheusden, W.L. Warren, C.H. Seager, D.R. Tallant, J.A. Voigt, B.E. Gnade, "Mechanisms behind green photoluminescence in ZnO phosphor powders", *J. Appl. Phys.*, **79** (1996) 7983–7990.
31. S. Monticone, R. Tufeu, A.V. Kanaev, "Complex nature of the UV and visible fluorescence of colloidal ZnO nanoparticles," *J. Phys. Chem. B*, **102** (1998) 2854–2862.